# MULTIPULSE POTENTIODYNAMIC STUDIES OF LOW MOLECULAR WEIGHT HYDROCARBONS ON SEMIMICRO FUEL CELL ELECTRODES

L.W. Niedrach

General Electric Research Laboratory
Schenectady, New York

## INTRODUCTION

Because of the limitations on the amount of information that can be obtained from polarization curves and material balances, it was felt desirable to study the behavior of hydrocarbon fuel cell anodes with multipulse potentiodynamic (MPP) techniques such as have been developed for microelectrodes(1,2). An additional purpose of the work was to compare observations upon fuel cell electrodes with similar observations with platinum wire microelectrodes. Such a comparison, which has been made in the case of ethane, has been described elsewhere(3).

In the course of fuel cell work it has been observed quite generally that the performances of all saturated hydrocarbons are similar although trends are evident as the molecular weight is changed. For this reason the three simplest hydrocarbons, methane, ethane, and propane, were used in this study as model compounds, and the more detailed work was confined to the first two fuels. A miniature version of a previously described(4) "conducting-porous-Teflon" fuel cell electrode (containing platinum black as the catalyst) was employed.

## EXPERIMENTAL

A three-compartment, Teflon cell described elsewhere(3) was used in these experiments. The working electrode consisted of a 0.2 cm diameter Teflon-bonded, platinum black electrode(4). Both the hydrogen reference and the counter electrodes were platinized platinum flags. The former communicated with the working anode through a Luggin capillary. The cell was operated in an air thermostat, enabling control of temperature to within 0.1°C.

The 4.3 N perchloric acid electrolyte solution used for this work was prepared from reagent grade perchloric acid and quartz distilled water. Electrolytic grade hydrogen was used in the reference electrode chamber, and Phillips research grade hydrocarbons were used as the fuels. Tank argon, deoxygenated by passage over heated copper turnings, was used as the "fuel" for obtaining solvent blanks. Tank argon was also used for degassing the solution.

The electronic instrumentation and circuit have been described previously(1).

The potential-time sequence applied to the anode for adsorption studies at constant potential is shown in Fig. 1. The significance of the steps is covered below.

A. Pretreatment step (15 sec) to remove oxidizable impurities and to produce a layer of "adsorbed oxygen" which serves to block fuel adsorption. The solution is vigorously stirred and purged with argon to remove molecular oxygen and oxidation products formed.

B. Potential step, during which the oxygen layer formed in (A) is maintained, and the solution is purged for an additional 1 minute. The solution is then allowed to become quiescent for 1 minute.

C. Reduction step (15 sec) during which the "adsorbed oxygen" layer is completely reduced within the allotted time. At this low potential (0.06 volt) the adsorption of the hydrocarbons is blocked. This step was included so that the reduction of the surface and the adsorption of the hydrocarbon would not occur simultaneously. However, omission of this step was found to have no detectable effect on the equilibrations, except for an initial current transient.

D. Adsorption step, during which the hydrogen from (C) is rapidly oxidized, exposing a reproducibly clean surface for adsorption. The duration of this step is the adsorption time, $T_D$*.

E. Anodic sweep at 0.1 v/sec. The adsorbed fuel is oxidized and the surface covered with a layer of "adsorbed oxygen". Subtraction of the charge due to surface oxidation from the total charge yields the charge, $Q_E$, required to oxidize the surface species derived from the adsorbed fuel.

E'. Alternative to (E), a cathodic sweep at 0.025 v/sec. which is used for determination of the "real" surface area of the electrode from the charge ${}_SQ_H$ corresponding to hydrogen deposition. In this case, argon is substituted for the hydrocarbon fuel.

When the sequence of Fig. 1 is terminated in Step (E') (linear cathodic sweep) a "hydrogen-deposition" trace may be obtained. From the charge, ${}_SQ_H$, associated with this trace, the "real" area of the electrode may be derived(1). In the present work ${}_SQ_H$ was determined using a sweep rate of 0.025 v/sec. Over the useful range of v = 0.01 to 0.1 v./sec., ${}_SQ_H$ has been found reproducible to within 5% for this type of electrode(3). In calculating the "real" area of the electrode 0.21 mcoul/cm$^2$ was assumed to be the charge associated with one square centimeter(5).

For the determination of the charge, $Q_E$, associated with the oxidation of the adsorbed hydrocarbon species, the sequence of Fig. 1 terminating in step (E)(linear anodic sweep) was used. When argon is serving as the "fuel" the application of the pulse sequence to an electrode results in an "oxygen adsorption" trace. When a similar sequence is employed following an equilibration with a hydrocarbon fuel, a trace corresponding to oxidation of the fuel as well as the electrode surface is obtained. The closed area defined by the two traces may be used for the determination of $Q_E$.(1) Actually the closed area corresponds to charge, $Q_{E'}$, which may include several terms:

$$Q_{E'} = Q_E + Q_{E''} + \Delta Q_{cap.} + \Delta Q_o \qquad (1)$$

where $Q_E$ = charge corresponding to oxidation of the hydrocarbon fuel adsorbed on the surface during step (D).

*The subscript here and for other time intervals refers to the step involved according to Fig. 1.

$Q_{E''}$ = charge corresponding to fuel not adsorbed during step (D) but which oxidizes during step (E) with or without a preceding adsorption step.

$\Delta Q_{cap.}$ = Difference in capacitive charges included under the "oxygen adsorption" and "fuel" traces due to differences in initial surface states.

$\Delta Q_o$ = Difference in charges due to surface oxidation, included under "oxygen adsorption" and "fuel" traces.

It has previously been demonstrated, with ethane on smooth platinum,(2) that $Q_{E'} \simeq Q_E$ if $\underline{v} < 20$ v/sec. At higher values of $\underline{v}$, $Q_{E'} < Q_E$, at least partially because some of the adsorbed fuel is retained on the surface during sweep (E). At the other end of the scale, it is important that the sweep speed not be so slow that appreciable readsorption of the fuel occur during step (E), and cause $Q_{E''} > 0$. For the present electrode the useful range of $\underline{v}$ was examined by adsorbing a fixed amount of ethane (corresponding to $T_D$ = 600 sec) and measuring $Q_{E'}$ for a range of sweep speeds(3). The useful range was found to extend from approximately 0.1 to 0.4 v/sec., and in this range we assume $Q_E = Q_{E'}$. A sweep speed of $\underline{v}$ = 0.1 v/sec was used routinely in the present work.

Polarization curves were obtained in two ways. The first method involved application of Steps (A-D) of Fig. 1 before each measurement of current at a particular potential U. In the second method, steps (A-D) of Fig. 1 were applied only once, at the lowest values of U. The potential was then changed in increments and the current recorded for each potential after an apparent constant value was established. The two methods gave essentially identical results.

RESULTS

Traces obtained during linear anodic sweeps (l.a.s.) are shown in Fig. 2 for methane, ethane, and propane after equilibrations at 60°C at 0.3 and 0.4 volt. An argon blank is also included for comparison purposes. The ethane and propane show two types of oxidation waves. Wave 1 occurs at potentials below which (approx. 0.8 v) the electrode surface is itself oxidized. This first wave generally exhibits a well-defined peak. The second wave is more diffuse and extends all the way from approximately 0.8 volt to oxygen-evolution potentials. Methane differs markedly in that only wave 1 can be detected during oxidation of the ad-layer. Similar structures have been observed for the oxidation waves obtained for ethane adsorbed on platinum wire micro electrodes(2,6). These results imply a range of reactivities for a variety of ad-species on the electrode surface.

The adsorption of methane and ethane has been examined over a wider range of potentials than are shown in Fig. 2. In both cases a maximum value of $Q_E$ occurs around 0.3 v. Below 0.1 volt, both adsorptions become negligible because of suppression by hydrogen on the surface. At potentials above 0.5 volt no ad-layer is observed for methane because of rapid oxidation following adsorption. Wave 1 for ethane becomes negligible at potentials above 0.6 volt and Wave 2 at potentials above 0.9 volt. The former wave, like that for methane, disappears because the ad-species associated with it are oxidized as rapidly as they appear on the surface. The latter wave disappears at the higher potentials because of rapid oxidation as well as

suppression of the adsorption rate.

Attempts to obtain similar data for ethylene with the Teflon-bonded electrodes have been unrewarding. Rates of adsorption are excessive for the low scan rates permissible with these electrodes, and readsorption prevents the accurate measurement of $Q_E$. With platinum wire microelectrodes, however, Gilman(6) has demonstrated that adsorbed ethylene and acetylene show only wave 2 at 60°C.

The effect of equilibration time on the l.a.s. traces for methane and ethane adsorbed at 0.3 volt is shown in Fig. 3. At 65°C, the single wave is evident for methane for equilibration times as long as one hour. In the case of ethane at 60°C, the ratio of the charges associated with wave 1 and wave 2 is not a sensitive function of the adsorption time. At 0.3 volt about 45% of the charge is associated with wave 1, and this value prevails up to a potential of 0.5 volt. At higher potentials the ratio declines rapidly.

At 0.3 volt, $Q_E$ initially varies linearly with time but subsequently becomes linear with the logarithm of time for both methane and ethane. At 65°C the maximum (initial) adsorption rate for methane in terms of $\Delta Q_E/\Delta t$ is approximately 0.00015 mcoul/sec/cm$^2$ of "real" area. For ethane at 60°C, $\Delta Q_E/\Delta t$ is approximately 0.010 mcoul/sec/cm$^2$. At 25°C the rate for ethane is approximately one tenth that at 60°C. The rate for ethane at 25°C is too low for reliable measurement with the present system.

Because of the slow adsorption of methane, even at 65°C, an hour is required at 0.3 volt before "steady-state" coverage is approached. In the case of ethane, however, "steady-state" is essentially achieved within 10 minutes at 60°C. At higher potentials, e.g., 0.4 to 0.6 volt, methane also approaches steady-state within 10 minutes (but with lower surface coverages). At these potentials ethane reaches steady-state within a few minutes. More detailed treatment of the kinetics of these adsorptions are given elsewhere(3,7).

Figures 4 and 5 show the effect of temperature on the l.a.s. traces for methane and ethane. Because ten minute equilibrations were used in all cases, the traces do not all correspond to "steady-state" coverages, particularly at the lower temperatures. It is pertinent to note, however, that the wave for methane grows in very rapidly as the temperature is raised. Similarly, wave 1 for ethane becomes more pronounced at the higher temperatures - in this case at the expense of wave 2.

The nature of the species associated with l.a.s. waves 1 and 2 is of considerable interest. In view of past observations that the material associated with the first wave is resistant to removal by cathodic hydrogenation(6,8) and is probably partially oxygenated(8), several additional experiments were undertaken. To demonstrate that related, partially oxidized species do indeed oxidize further on the Teflon-bonded electrodes at 60°C over the same potential range as wave 1, the data in Fig. 6 were obtained. For this purpose, the electrode was equilibrated with CO (at 0.3 volt), $CO_2$ (at 0.06 and 0.2 volt) and argon saturated with formic acid vapor at 25°C (at 0.06 and 0.2 volt) prior to the l.a.s. It was further observed that the surface species from these equilibrations were not removed by cathodic hydrogenation.

To determine whether some of the species of wave 1 are removable by cathodic hydrogenation, and therefore probably unoxygenated, additional cathodic hydrogenations were performed after equilibrations of the electrode with methane and ethane at several potentials. In these experiments sequence A-D of Fig. 1 was first followed. After adsorption for time, $T_D$, the potential was again stepped down to 0.06 volt for 2 to 5 minutes before application of the linear anodic sweep. The results of these experiments are summarized in Fig. 7 and Table I. It is clear that in each case a portion of the surface species was removed by this treatment. The amount removed decreased with increasing equilibration potential. In the case of the ethane all of wave 2 was removed by the hydrogenation treatment. The present results for ethane differ from those of Gilman(2) who performed similar hydrogenations with the wire microelectrode after equilibrations at 0.4 volt. In that case no desorption of wave 1 species was observed after hydrogenation at 0.06 volt. The diffuse structure of the Teflon electrode as well as small differences in the catalytic behavior may account for the observed differences.

Table I

Effect of Cathodic Hydrogenation on Wave 1
($T_D$ = 5 min; $T_{Hyd}$ = 5 min)

| | Methane 65°C | | Ethane 60°C | |
|---|---|---|---|---|
| | 0.3 volt | 0.4 volt | 0.3 volt | 0.4 volt |
| $Q_E^1$ = initial; mcouls | 4.0 | 2.8 | 10.1 | 8.0 |
| $Q_E^1$ = after hydrogenation; mcouls | 2.5 | 2.3 | 3.8 | 5.5 |
| $\Delta Q_E^1$, mcouls | 1.5 | 0.5 | 6.3 | 2.5 |
| per cent removed | 38 | 18 | 62 | 31 |

Another aspect of the problem that was given attention was the relationship between surface coverage and the polarization curves for methane and ethane. Such data for the two fuels, obtained at 65° and 60°C, respectively, are shown in Figs. 8 and 9. In these figures the abscissa is expressed in terms of the current density per $cm^2$ of "real" and "geometrical" area of the electrode. Therefore, the data may be related to the adsorption studies as well as performance curves for operating fuel cell devices.

The form of the polarization curves is typical of those for a variety of fuels when the data are obtained potentiostatically. Even hydrogen shows the minimum in the region from 0.9 to 1.4 volt on smooth platinum. Over the potential range from 0.3 to 0.45 volt, the curve for ethane has a linear Tafel region with a slope of 0.066 v/decade of current.

The surface coverages in these figures are expressed in terms of the charge per square centimeter of "real" area. The charge, $Q_E^1$ refers to that associated with wave 1, and in the case of ethane, $Q_E$ refers to the total charge associated with the combined species of waves 1 and 2.

DISCUSSION

Among the present observations, those of most significance with regard to the performance of practical fuel cell anodes are the marked effects of temperature on the rates of adsorption and on the nature of the surface species as indicated by the l.a.s. traces. In the case of ethane, a ten-fold increase in the initial adsorption rate on a "clean" surface occurs in going from 25° to 60°C. A similar factor applies to the partially covered surface. The effect of tmeperature on the corresponding adsorption rate formethane appears to be even more pronounced although reliable data could not be obtained at 25°C. Such pronounced temperature coefficients for the adsorptions are reflected in the observed improvement in performance of hydrocarbon fuel cells with increasing temperature. In particular, they relate to the regions of "unstable" performance observed with saturated hydrocarbon fuel cells operating on resistive load.(9-11) Under these conditions, it will be recalled that at low current densities steady performance is obtained while at higher current densities the performance decays with time or, under certain conditions, oscillations set in(11,12). As a result of the increasing adsorption rates with increasing temperature, the region of instability occurs at continuously higher current densities as the operating temperature is increased.

When polarization curves are obtained potentiostatically, as in the present work, maximum currents are observed in place of the instability associated with resistive loads. It is of interest to compare the values of the maximum currents in Figs. 8 and 9 with those calculated from the observed adsorption rates on clean surfaces as measured at 0.3 volt.

In converting the adsorption rates to equivalent current densities, it must be recalled that the former are expressed in terms of the change in surface charge with time, $\Delta Q_E/\Delta t$. Allowance must therefore be made for any oxidation that occurred during the adsorption step itself; e.g., immediate oxidation of dissociated hydrogen. This may be done by multiplying $\Delta Q_E/\Delta t$ by the ratio of the charge associated with the hydrocarbon fuel molecule to that of the adsorbed species.

While the precise composition of the ad-layer has not been established for either methane or ethane, especially after short equilibrations, it is possible to calculate a range of limiting currents from the adsorption data at 0.3 volt. In the case of methane, depending upon whether the ad-layer is assumed to have an average composition approaching that of methyl radicals or that of a highly oxygenated species such as CO, the observed rate of adsorption would be equivalent to a steady state current density of from 0.15 to 0.6 microamps/$cm^2$ of "real" area. The observed value of 0.3 microamps/$cm^2$ is in good agreement in view of the evidence for a mixture of $C_1$ radicals and partially oxygenated species.

For ethane it is reasonable to bracket the composition of the ad-layer between one corresponding to $C_2H_2$ radicals and one corresponding to CO. This gives a range of current densities from 14 to 35 microamps/$cm^2$. In this case the observed maximum current of 2.5 microamps/$cm^2$ is much lower than the calculated value. This undoubtedly reflects the fact that at the potential of the maximum "steady-state" current some of the more refractory species are present on the surface and lower the adsorption rate relative to that on the "clean"

surface at 0.3 volt. The decline in the current density that occurs at higher potentials appears to reflect further reductions in adsorption rates as a result of such processes as "surface oxidation", anion adsorption, and stronger bonding of water to the surface. These processes would also contribute to the similar decline in methane performance at the higher potentials.

At low potentials, the effect of the adsorption rate on the polarization curve is minimal. Here it is clear that the overvoltage required for the further oxidation of surface intermediates to $CO_2$ is limiting. This is true, of course, under potentiostatic conditions as well as with the resistive loads of practical fuel cells.

With regard to specific mechanisms for the oxidation reactions, it would be premature to attempt to discuss them in any detail at this time. It is appropriate, however, to consider briefly some of the possible paths suggested by the available information. In particular, it is pertinent to speculate about the meaning of the two separate l.a.s. waves seen with ethane and propane, the single wave seen with methane, and the evidence for the partially oxidized surface species. In the discussion that follows, ethane will be used as the model with the expectation that higher molecular weight hydrocarbons will behave similarly. The behavior of methane, in turn will be somewhat simpler.

The initial step must certainly involve adsorption of the fuel on the electrode surface. On the basis of careful kinetic studies with ethane on wire microelectrodes, Gilman has concluded(6) that this primary adsorption step corresponds to the formation of an "ethyl radical" on the surface. This may be represented by

$$(1) \quad C_2H_6(gas)^* + S \rightarrow S\text{-}C_2H_5 + H^+ + e$$

at potentials at which appreciable currents are drawn from the electrode. He points out that an equivalent route is given by

$$(1a) \quad C_2H_6(gas) + 2S \rightarrow S\text{-}C_2H_5 + S\text{-}H$$

in which case the adsorbed hydrogen is rapidly consumed by the Volmer reaction:

$$(1b) \quad S\text{-}H \rightarrow S + H^+ + e.$$

At low potentials, of course, some of the hydrogen will remain adsorbed on the surface.

Gilman then reasons that the ethyl radical follows two paths. The first results in the formation of four surface bonds to the surface without rupture of the C-C linkage:

$$(2) \quad S - C_2H_5 + 3S \rightarrow S_4 - C_2H_2 + 3H^+ + 3e.$$

---

*More precisely, the gas will first dissolve in the electrolyte and be transported by diffusional processes to the electrode where it will adsorb from solution. While mass transport processes are not limiting in the work under discussion, it is obvious that they can become important under some conditions of operation. For practical fuel cell electrodes it is important that mass transport limitations be minimized.

This species is associated with wave 2 obtained with a l.a.s. and is identical with the single adsorbed species obtained when ethylene and acetylene are adsorbed(6). The present work is in accord with this interpretation, and cathodic hydrogenations of adsorbed ethane at 25°C have shown that the major material on the surface at that temperature corresponds to $C_2$ species, while those for propane correspond to $C_3$ species(8).

The second reaction path of the ethyl radical results in the formation of the material associated with wave 1, which Gilman also obtained for ethane on the platinum wire microelectrode. This wave he found, in contrast to wave 2, to be resistant to cathodic hydrogenation. He has also found that the species associated with wave 2 do not readily convert to those of wave 1.(6) In the absence of detailed kinetic data for the species associated with wave 1 Gilman did not speculate in detail on its identity.

The new data obtained with the Teflon-bonded electrodes are helpful in this area. The similarities between the single wave for methane and wave 1 for ethane strongly suggest that the second reaction path of the ethyl radical involves C-C bond fission as indicated in the following general equation:

$$(3) \quad S\text{-}C_2H_5 + S \rightarrow 2S - CH_a + (5-2a)\ H^+ + (5-2a)\ e.$$

This is in accord with the previous observation that $C_1$ species form during ethane (and propane) adsorption even at 25°C.(8) Grubb has also observed that on open circuit appreciable amounts of methane desorb from propane anodes in fuel cells operating at 65°C.(14) (The methylene radical with two carbon bonds to the surface may represent the principal species in parallel with the $C_2H_2$ of wave 2 which also has two surface bonds per carbon atom.)

The $C_1$ species in turn appear to react readily with water to form a partially oxygenated material which corresponds to the previously proposed "CO-like" species of Niedrach(8) and the "reduced $CO_2$" of Giner(15), and which Giner has also more recently found to be formed during the oxidation of hydrocarbons(16). The specific identity of the oxygenated species is as yet unknown and the reaction can therefore best be represented by:

$$(4) \quad S\text{-}CH_a + b\ H_2O + cS \rightarrow S_{(c+1)} - CH_dO_b + (a + 2b-d)\ H^+ + (a + 2b-d)e.$$

That both the $C_1$ species and the partially oxygenated species are present on the surface and oxidize over the same potential range is indicated by the new hydrogenation experiments with methane and ethane. Since Eq. (3) represents a "cracking" reaction, and Eq. (4) a "reforming" reaction, these observations suggest that it would be profitable to direct attention toward the study of the behavior of alternative catalysts in promoting such reactions.

With regard to the more refractory species of wave 2, which oxidize only at higher potentials, it is likely that an entirely different mechanism of oxidation prevails. This conclusion is based upon Gilman's observation that conversion to the species of wave 1 is slow(6). It is therefore likely that oxidative attack occurs before the C-C bonds are ruptured. This could result in the formation of alcohol-like species as intermediates. It should be emphasized, however, that such intermediates will undoubtedly be quite distinct from

those involved in the direct oxidation of alcohol-type fuels at moderate temperatures. The alcohol-like species derived from hydrocarbons would be strongly bound to the surface by multiple carbon-metal linkages, and hence complete oxidation to $CO_2$ would be assured. With alcohol fuels it is more likely that weaker bonds between the oxygen and the metal are involved. This is suggested by the incomplete oxidation to organic acids that is often observed with alcohols(17) at moderate temperatures. It is further supported by the behavior of alcohols towards deuterium exchange, where it is found that the hydroxylic hydrogen undergoes exchange most readily(18).

## CONCLUSIONS

The behavior of saturated hydrocarbons on platinum catalyzed fuel cell anodes is strongly influenced by the rate of adsorption and the ability of the catalyst to promote "cracking" of C-C bonds as well as the reaction of $C_1$ radicals with water. Both the rate of adsorption and the catalytic activity of the platinum have pronounced positive temperature coefficients.

Species present on the electrode surface include $C_1$ radicals and partially oxygenated $C_1$ species in all cases. In the case of ethane and higher hydrocarbons multicarbon species are also present. These are strongly bound to the surface by multiple carbon-metal bonds and are relatively refractory.

After a primary adsorption step, at least two distinct reaction paths are followed by ethane and higher hydrocarbons. One path results in the formation of the relatively refractory species. The more desirable path results in "cracking" of the carbon chain to form the $C_1$ radicals and the partially oxygenated species.

Catalysts for hydrocarbon anodes should promote the cracking of higher molecular weight hydrocarbons to form $C_1$ radicals and also promote the reaction of these fragments with water.

In view of the many species present on the electrode surface and the changes in coverage and composition with temperature, potential, and time, much attention to analytic detail will be required before a definitive mechanism can be derived. All of these factors must be considered in valid interpretations of electrochemical performance data.

## ACKNOWLEDGMENTS

The author is indebted to S. Gilman for many helpful discussions, and to I. Weinstock who provided some of the data.

This work is a part of the program under contracts DA-44-009-AMC-479(T) and DA-44-009-ENG-4909, ARPA Order No. 247 with the U.S. Army Engineer Research and Development Laboratories, Ft. Belvoir, Virginia, to develop a technology which will facilitate the design and fabrication of practical military fuel cell power plants for operation on ambient air and hydrocarbon fuels.

## REFERENCES

1. S. Gilman, J. Phys. Chem., 67, 78 (1963).
2. S. Gilman, Electrochemical Society Washington Meeting, October 1964, Extended Abstracts of the Battery Division, p. 72;

Trans. Far. Soc., in press.
3. L.W. Niedrach, S. Gilman, and I. Weinstock, J. Electrochem. Soc., to be published.
4. L.W. Niedrach and H.R. Alford, J. Electrochem. Soc., 112, 117 (1965).
5. F.G. Will and C.A. Knorr, Z. Elektrochem., 64, 258 (1960).
6. S. Gilman, preprint, this meeting.
7. L.W. Niedrach, to be published.
8. L.W. Niedrach, J. Electrochem. Soc., 111, 1309 (1964).
9. W.T. Grubb, Proc. 16th Annual Power Sources Conference, Atlantic City, N.J., p.31 (1962).
10. L.W. Niedrach, J. Electrochem. Soc., 109, 1092 (1962).
11. M.J. Schlatter, in "Fuel Cell Systems" (R.F. Gould, ed.), p.292. Advances in Chemistry Series 47, American Chemical Soc., Washington, 1965.
12. H. Binder, et al., J. Electrochem. Soc., 112, 355 (1965).
13. S. Gilman, J. Phys. Chem., 67, 1898 (1963).
14. W.T. Grubb, J. Electrochem. Soc., 111, 1086 (1964).
15. J. Giner, Electrochimica Acta, 8, 857 (1963).
16. J. Giner, 15th Meeting CITCE, London and Cambridge, September 21-26, 1964, summaries of papers, p. xxix.
17. H. Binder, et al., in "Fuel Cell Systems" (R.F. Gould, ed.) p.283. Advances in Chemistry Series 47, American Chemical Soc., Washington, 1965.
18. G.C. Bond, "Catalysis by Metals", Academic Press, New York, (1963) p.220.

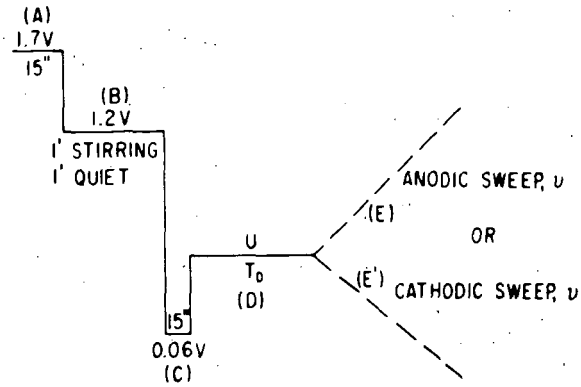


FIG. 1 POTENTIAL SEQUENCES APPLIED TO THE TEST ELECTRODE.

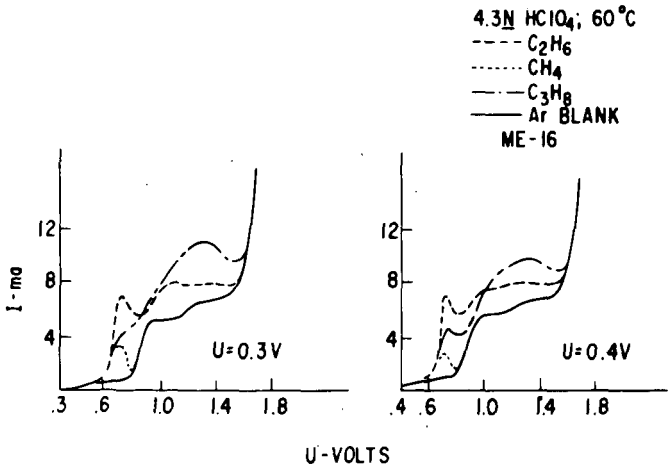


FIG. 2 CURRENT-POTENTIAL (TIME) TRACES FOR SEVERAL HYDROCARBON FUELS AFTER EQUILIBRATION AT DIFFERENT POTENTIALS.

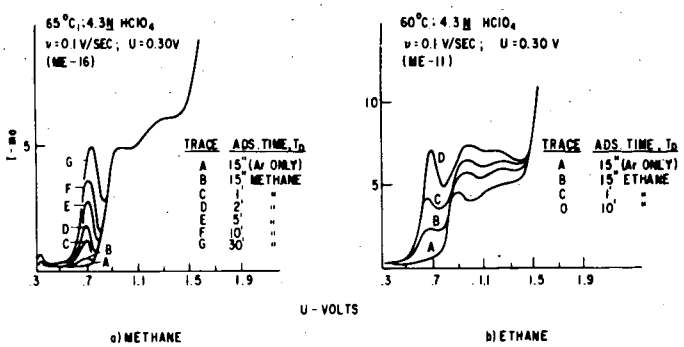


FIG. 3 CURRENT-POTENTIAL (TIME) TRACES FOR METHANE AND ETHANE AFTER DIFFERENT ADSORPTION TIMES.

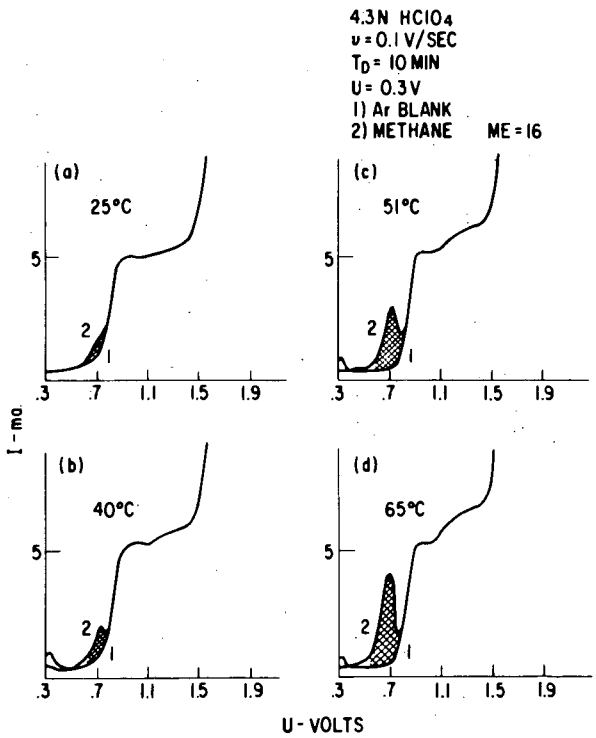


FIG. 4 CURRENT-POTENTIAL (TIME) TRACES FOR METHANE ADSORBED AT SEVERAL TEMPERATURES.

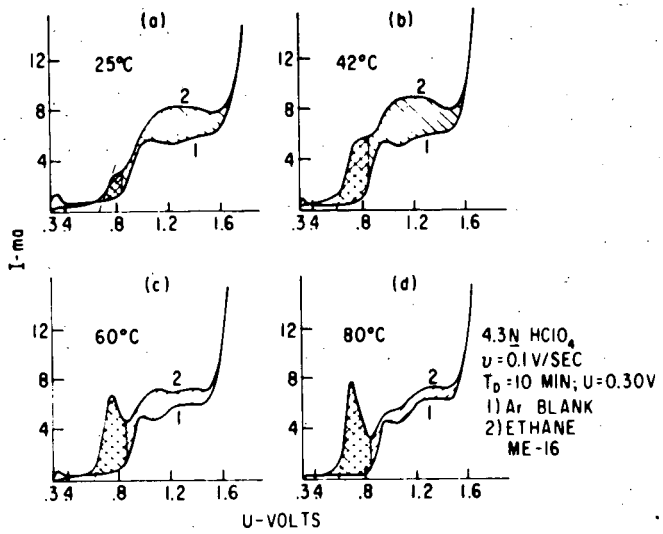


FIG. 5 CURRENT-POTENTIAL (TIME) TRACES FOR ETHANE ADSORBED AT SEVERAL TEMPERATURES.

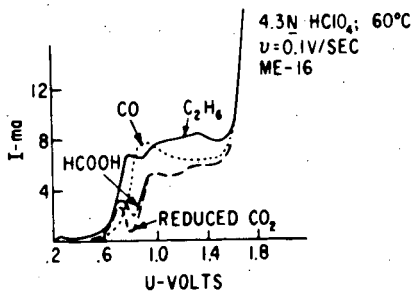


FIG. 6 CURRENT-POTENTIAL (TIME) TRACES FOR SEVERAL CARBONACEOUS MATERIALS ADSORBED ON PLATINUM.

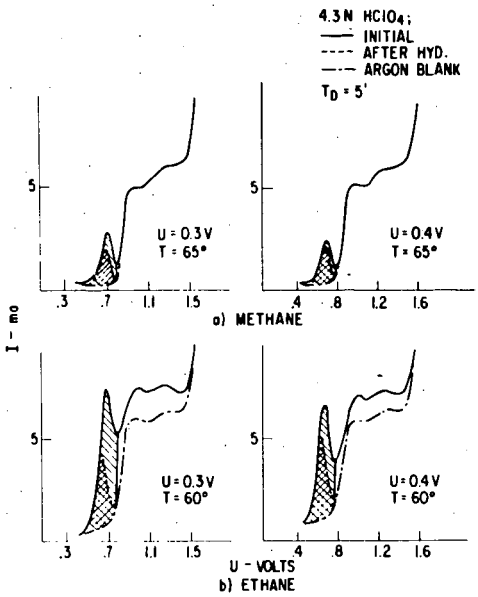


FIG. 7 EFFECT OF CATHODIC HYDROGENATION ON THE CURRENT-POTENTIAL (TIME) TRACES FOR ADSORBED METHANE AND ETHANE.

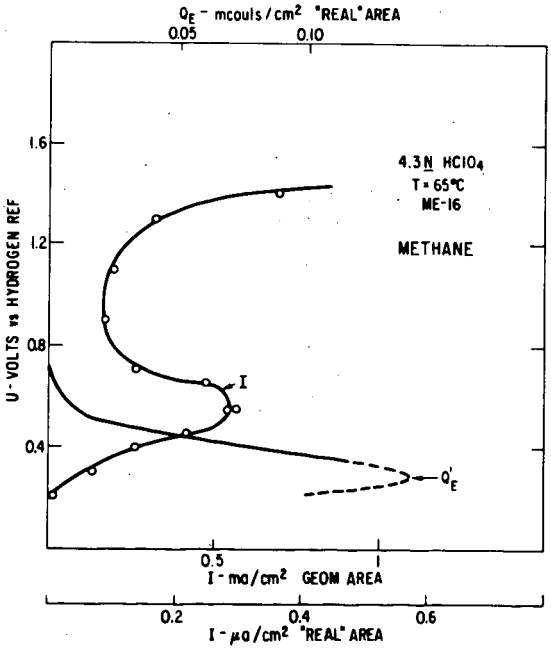


FIG. 8 POLARIZATION AND SURFACE COVERAGE CURVES FOR METHANE

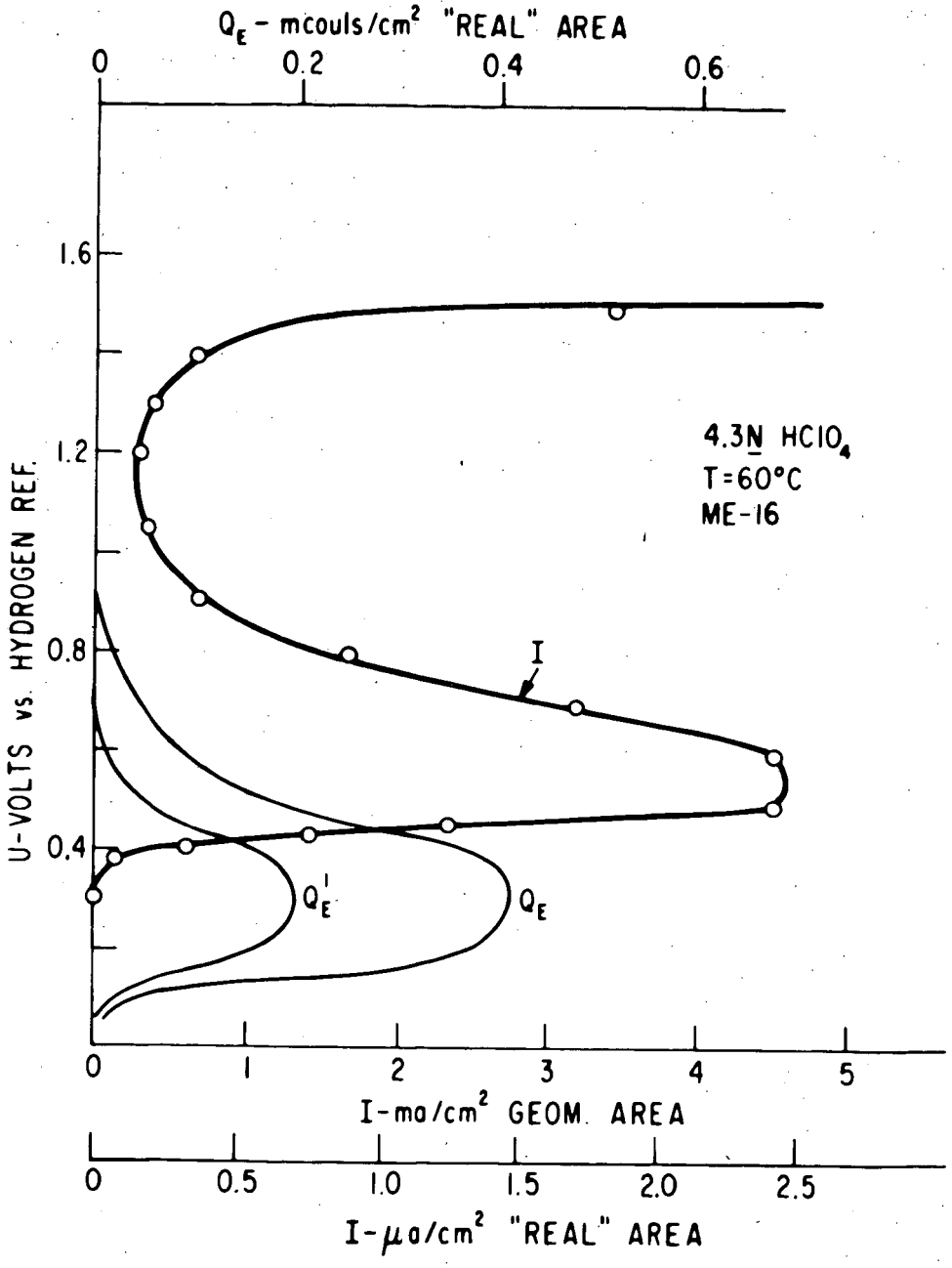


FIG. 9 POLARIZATION AND SURFACE COVERAGE CURVES FOR ETHANE.